Directed assembly of one-dimensional magic cluster arrays by domain boundaries

Andrew G. Mark* and A. B. McLean†

Department of Physics, Engineering Physics, and Astronomy, Queen's University, Kingston, Ontario, Canada K7L 3N6

(Received 5 May 2011; revised manuscript received 21 April 2012; published 24 May 2012)

The most commonly occurring boundary separating Ge-5 × 5 domains grown on Si(111) is the B[$\bar{2}$ 2] domain boundary. We demonstrate that this boundary can be used to template one-dimensional arrays of identical In and Ga magic clusters with a lattice constant of 3.3 nm. This is larger than the lattice constant of the two-dimensional magic cluster arrays templated by the Si(111)-7 × 7 surface reconstruction (2.7 nm), although the magic clusters have the same structure. We also demonstrate that a necessary condition for cluster growth at the domain boundary is the presence of faulted dimer-adatom-stacking-fault-7 × 7 half unit cells. The relatively unexplored possibility of exploiting the unique structural and electronic properties of domain boundaries in nanostructured materials is discussed.

DOI: 10.1103/PhysRevB.85.195448 PACS number(s): 81.16.Rf, 68.35.Dv, 68.43.Hn, 81.16.Dn

It is well known that crystalline surfaces can serve as templates to direct the assembly of nanostructured arrays from individual atoms or molecules.[1–9] A strength of the templating methodology is that it is a parallel process that obviates the need for time-consuming serial assembly. For this reason, templating is frequently used in the search for nanostructured materials for electronic and photonic applications.[3,10] There is also interest in the development of templating strategies for one-dimensional (1D) nanostructures, for example, using steps on vicinal surfaces,[11] because 1D nanostructures hold the promise of novel electronic[12,13] and magnetic[14,15] properties.

An excellent example of 2D templating is the well-known magic cluster phase that forms when group-III elements (In,[1,16–18] Ga,[17,19,20] and Al[17,21,22]) and also some other elements from outside of this group[16,23–26] are added to Si(111)-7 × 7. A scanning tunneling microscope (STM) image of the In/Si(111)-7 × 7 magic cluster phase is presented in Fig. 1(a). In a more conventional nucleation and growth scenario,[27,28] the surface would contain clusters of different sizes, but here, six In adatoms and the three edge or middle Si adatoms combine to reconstruct the center of the half unit cell (HUC). This *local* reconstruction saturates the dangling bonds in the center of the HUC and the atomic number distribution for the clusters is strongly peaked at six. The magic clusters also prefer to form in the faulted HUC (FHUC)[16,29] [see Fig. 1(a)]. When all the FHUCs on the surface are occupied, the result is a 2D hexagonal cluster array with a lattice constant of 2.7 nm, defined by the underlying 7 × 7 lattice which survives the reconstruction of the HUCs.[1,16–18]

Attempts to extend this technique to other dimer adatom stacking fault (DAS) reconstructions, and thereby create arrays with different periodicities, have so far proven unsuccessful. For instance, the clusters that grow on Si(111)-Ge(5 × 5) possess a variety of irregular forms of undetermined structure that span the dimer rows between HUCs.[30] So scaling the reconstruction's unit cell dimensions does not trivially change the cluster spacing.[31]

As mentioned above, the atomic steps on vicinal surfaces can serve as a template for directing the growth of 1D nanostructures. On semiconductor surfaces, an important breakthrough was the demonstration that vicinal offcuts could be used to generate regular step arrays with exceptional structural quality.[11] These step arrays possess a low concentration of structural defects, such as kinks,[32] that are commonly found on low index semiconductor surfaces. Because of this, vicinal surfaces have been used as patterns for nanowires[14,33,34] and 1D nanocluster arrays.[35] For good reason, few attempts have been made to use the boundary that separates different domains on a surface[36,37] as a template. Although these extended defects have long been recognized as special sites for preferential nucleation,[38–40] domain boundaries that are both atomically ordered and straight are very rare.[41] Furthermore, to use domain boundaries as templates it would be advantageous for the templated species to dewet the domains and decorate the domain boundary regions. Finding a system with all of these properties is a formidable challenge.

The purpose of this paper is to demonstrate that, even although it is presently impossible to control the distribution of domain boundaries on the Si(111)-Ge system, the boundaries between 5 × 5 domains of *a particular type or character* can be used to direct the growth of both In and Ga into 1D magic cluster arrays. This effect is particularly striking because the 5 × 5 domains act as sources of In or Ga atoms; there is mass transport from the 5 × 5 domains to the domain boundaries leading to decoration of the boundary regions. These arrays that subsequently form at the domain boundaries are 1D with a lattice constant of 3.33 nm. Consequently, *they have reduced dimensionality and increased spacing compared to those found on* 7 × 7.

But before discussing the growth of clusters on 5 × 5 domain boundaries, we will describe cluster growth on surfaces that contain domains of both 5 × 5 and 7 × 7. Such multiphase surfaces were prepared by solid phase epitaxy (SPE), where Ge—in this case a subbilayer coverage of 0.4 bilayers (BL)—was deposited onto a Si(111)-7 × 7 surface held at room temperature. This yielded an amorphous overlayer that when annealed for 15 min at ∼475 °C generated well-ordered islands of both 5 × 5 and 7 × 7 on 7 × 7 (Fig. 2).[42] Because Ge intermixes with Si,[43–47] the exact stoichiometry of the surface is unknown. Magic clusters were grown, according to a well established recipe[16,17,21] by exposing these surfaces to 0.01–0.07 ML (monolayers) of In or Ga with the substrate held at 150 °C. As is clear from the STM image presented in Fig. 2(b), In atoms form magic clusters on the 7 × 7

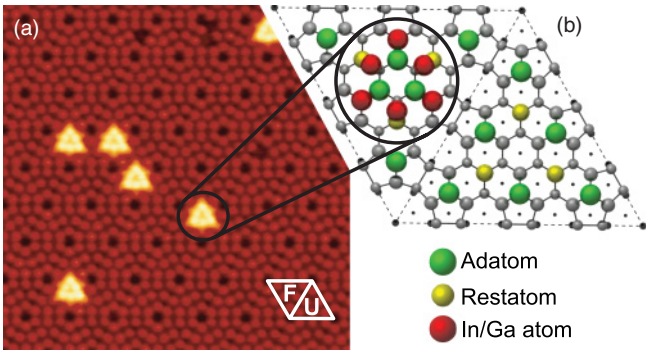

FIG. 1. (Color online) (a) STM image of In magic clusters on Si(111)–7 × 7 (22 × 22 nm^2; $V_S = +1.0$ V, empty states). The labels F and U indicate the position of the faulted and unfaulted 7 × 7 unit cell halves, respectively. (b) The accepted structure for the In magic cluster.[16] The lattice constant of the 7 × 7 unit cell, and hence the nearest neighbor spacing for FHUC clusters, is 2.7 nm.

domains, whereas the 5 × 5 domains are left bare. Ga behaves in the same manner, and in what follows, the behavior of In and Ga will be identical. Similar results have been reported for Ge clusters, although their structure differs substantially from the group-III clusters of interest here.[39] These results indicate that In forms magic clusters exclusively on the 7 × 7 reconstruction; that the differences between, and intermixing of, Ge and Si are less important than the structural differences between 7 × 7 and 5 × 5; and that adsorption of any type is inhibited on 5 × 5 relative to 7 × 7. This behavior will allow (see later) 5 × 5 domain boundaries to be decorated with magic clusters.

For cluster growth, the key structural features in each 7 × 7 HUC are the three restatoms and the three edge adatoms. In the cluster, each edge adatom displaces towards the center of the HUC and coordinates to the nearest restatoms through a metal atom [Fig. 1(b)]. This saturates six dangling bonds on the adatoms and restatoms, without changing the Si/Ge content of the HUC. On the other hand, each HUC of 5 × 5 contains three symmetrically equivalent adatoms, but only one restatom [Fig. 2(c)]. On this surface, the analogous magic cluster reduces the number of dangling bonds by only one, a

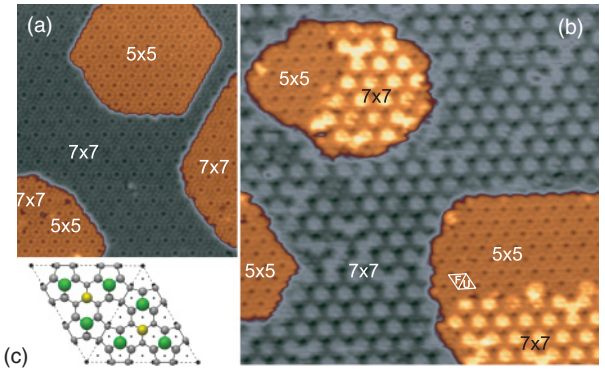

FIG. 2. (Color online) (a) A bare multiphase surface of Si(111)-Ge, containing islands of both 5 × 5 and 7 × 7, grown by SPE at ∼475 °C (33 × 55 nm^2, $V_S = +1.5$ V). (b) The same surface exposed to In. Magic clusters grow only on 7 × 7 domains (40 × 45 nm^2, $V_S = +1.5$ V). (c) Model for the 5 × 5 structure.

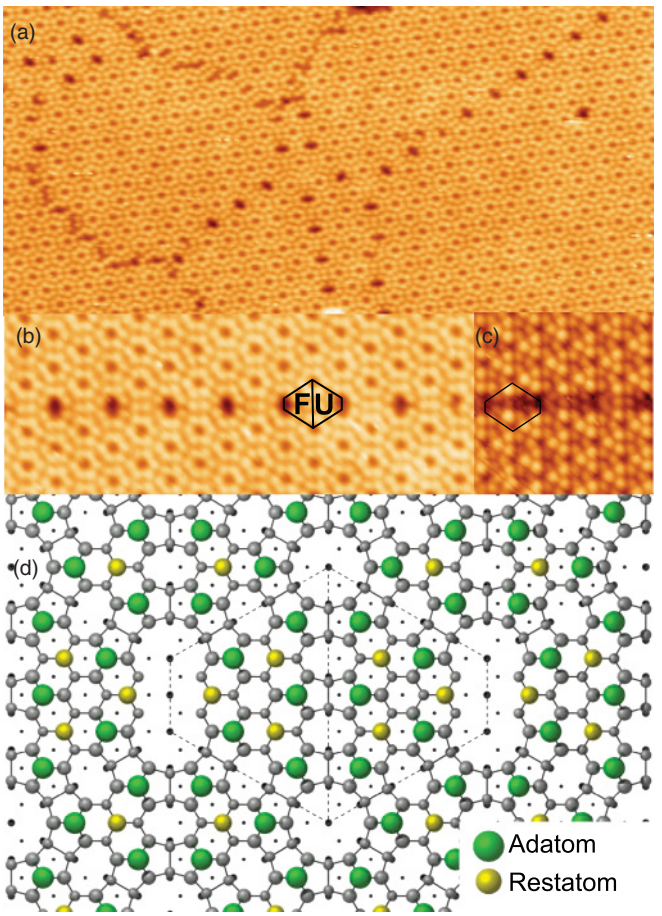

FIG. 3. (Color online) STM images of 5 × 5 domains and domain boundaries grown by Ge SPE on Si(111). (a) Domains of 5 × 5 (33 × 60 m^2, $V_S = +1.73$ V, empty states). (b) Empty and (c) filled state images of B[$\bar{2}$ 2] boundaries (10 × 27 nm^2, $V_S = +1.73$ V; 10 × 10 nm^2, $V_S = -1.50$ V). The boundary unit cells are outlined. (d) Atomic model of the B[$\bar{2}$ 2] boundary unit cell. The unit cell outlined by the dashed line is a truncated 7 × 7 unit cell that retains faulted (left) and unfaulted (right) half unit cells.

poor thermodynamic motivation, and requires the removal of two Si/Ge adatoms from the HUC, a strong kinetic inhibition.

Highly ordered domain boundaries were created to investigate their effect on cluster growth. In a manner similar to what was described above, SPE was used to prepare surfaces reconstructed exclusively as 5 × 5, by depositing Ge onto a room temperature substrate at a complete bilayer coverage followed by annealing at a higher temperature of ≈500 °C. As seen in Fig. 3(a), the high nucleation density on the amorphous intermediate leads to many domains of well-ordered 5 × 5.[42] Dividing the reconstruction domains is a network of boundaries, distinguished by the wide corner-hole like features. Several different types of boundaries are visible and these meet one another at kinks and vertices.

We have developed a nomenclature, based on the one introduced for 7 × 7 in Ref. 37, for indexing the 48 shift boundaries possible on 5 × 5.[48] Briefly, a boundary is identified by two parameters, its direction of propagation and the vector misfit between the two domains. A boundary is known as A type if it runs along the ⟨10$\bar{1}$⟩ family of directions,

and B type if it runs along one of the $\langle 11\bar{2}\rangle$ directions. Interestingly, boundaries that run along the latter directions do not appear on Si(111)–7 × 7.[37] The second parameter is the shift vector which describes the misregistration of one domain relative to the other, expressed in terms of the 2D surface unit vectors. Registration of the reconstruction with the substrate below means that the shift is restricted to 24 discrete possibilities. This is different from free graphene which can, in principle, adopt a continuum of possible shifts and tilts.[49] Together, the shift and translation vectors define the boundary conditions, and hence the atomic arrangement, for the narrow strip where two domains meet. Thus, the atomic structure that results for each unique combination of boundary parameters is itself unique, and we refer to it as *a boundary's character*. The long cool anneal at a temperature of 500 °C leads to many boundaries that are straight and uniform, and possess a well-defined unit cell. The dominant boundary type is the one shown in Figs. 3(b) and 3(c), which in our labeling scheme is B[$\bar{2}$ 2].

Figure 3(b) contains an empty-state STM image showing a straight and highly ordered structure that is characteristic of the achiral B[$\bar{2}$ 2] boundary.[48] The boundary unit cell has 10 adatoms in a truncated diamond arrangement separated from adjacent boundary cells by a deep, elongated corner hole. From filled-state images, such as Fig. 3(d), it is clear that the unit cell contains two inequivalent halves. The periodicity parallel to the boundary is that of the 5 × 5 domains: $5\sqrt{3}a = 3.33$ nm, where a is the ideal 1 × 1 Si(111) periodicity (0.384 nm), while at its widest point the unit cell has a width of $7a = 2.69$ nm.

The structure shown in Fig. 3(d) is constructed from DAS moieties so as to minimize the number of dangling bonds. It essentially consists of a truncated 7 × 7 unit cell, where the two adatoms at opposite ends of the unit cell have been removed and the corner hole expanded. The remaining 10 adatoms image as the bright protrusions in the empty state images. The stacking fault divides the cell into faulted and unfaulted HUCs resulting in the asymmetry observed in the filled state image. This model leaves additional dangling bonds on four dimer layer atoms, and three bulk atoms at the bottom of the boundary hole. Importantly, within each HUC, the 3 restatoms and remaining 5 adatoms are largely unchanged from their arrangement in native DAS-7 × 7.

When In or Ga is deposited on a surface with a high density of 5 × 5 domain boundaries, the interiors of the 5 × 5 domains remain largely unadorned, consistent with the dewetting of 5 × 5 described above. Instead, the metal segregates to the domain boundaries and, crucially, the degree of decoration depends on the character of the boundary. This is illustrated in Fig. 4 where both In and Ga magic clusters are found in the faulted half cells of the B[$\bar{2}$ 2] boundaries. The A-type boundaries are found to be bare and the few clusters that do form there (not shown) have irregular structure. In contrast, the B[$\bar{2}$ 2] boundary is densely covered with magic clusters.

The magic clusters found on B[$\bar{2}$ 2] domain boundaries are faithful reproductions of those found on 7 × 7.[16] For example, the different shapes of In and Ga clusters is duplicated. The more sp^3-like coordination of the corner In adatoms[17] leads to a triangular appearance for In clusters rather than the more compact shape seen for Ga [Figs. 4(b) and 4(c)]. This preservation of the cluster appearance is compelling

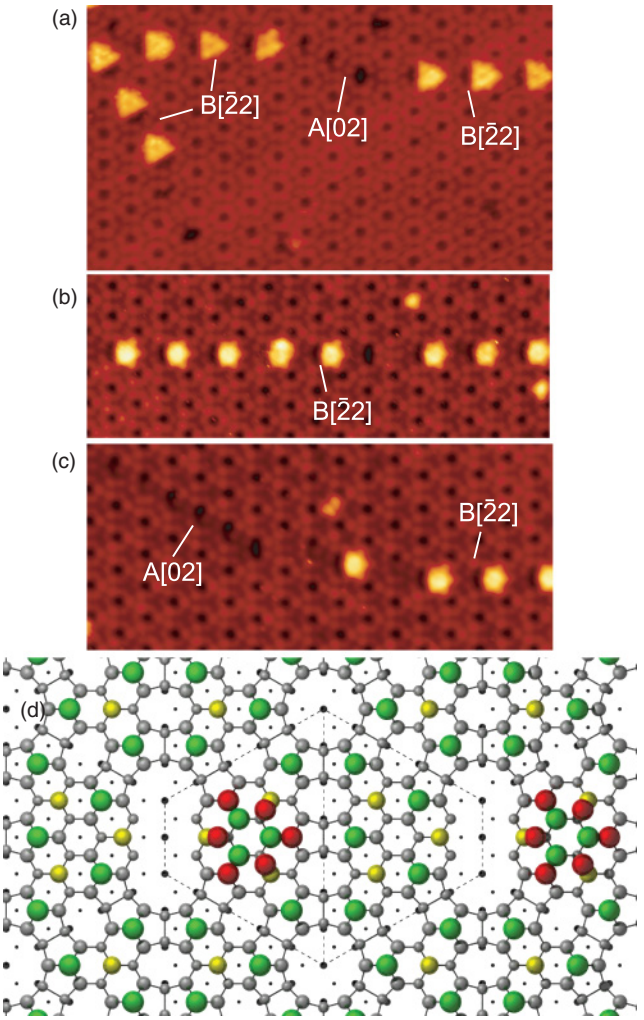

FIG. 4. (Color online) STM images of linear arrays of magic clusters grown on B[$\bar{2}$ 2] boundaries. (a) In clusters on two B[$\bar{2}$ 2] boundaries meet at a vertex near the top left of the image (16 × 28 nm^2, +1.79 V), (b) and (c) Ga clusters (10×30 nm^2, +2.46 V; 12 × 28 nm^2, +2.46 V). Note the bare A[0 2] boundaries. (d) Structure of B[$\bar{2}$ 2] boundary magic clusters.

evidence that clusters on the boundary share the same atomic arrangement as those on 7 × 7. The B[$\bar{2}$ 2] boundary, after all, is a strip of 7 × 7. Based on this, an atomic model, constructed by combining the model for B[$\bar{2}$ 2] [Fig. 3(d)] with the known structure for group-III 7 × 7 magic clusters,[16,50] is shown in Fig. 4(d). The clusters reduce the number of substrate Si/Ge dangling bonds from 23 per boundary unit cell to 17. The B[$\bar{2}$ 2] boundary thus templates a 1D array of magic clusters.

Conventionally, domain boundaries are regarded as special sites for nucleation due to the higher density of dangling bonds present there.[38–40] Indeed our structural models of the observed boundaries all have higher dangling bond densities than 5 × 5. But cluster growth on domain boundaries exhibits a preference for boundaries of different characters that goes beyond simple dangling bond density. As an example, consider the chiral A[0 2] boundary found in Figs. 4(a) and 4(c) which, unlike the adjacent B[$\bar{2}$ 2] segments, remains bare. The unit cell of this boundary is also a truncated half cell of 7 × 7 that differs from B[$\bar{2}$ 2] only in the details of the corner hole, and more

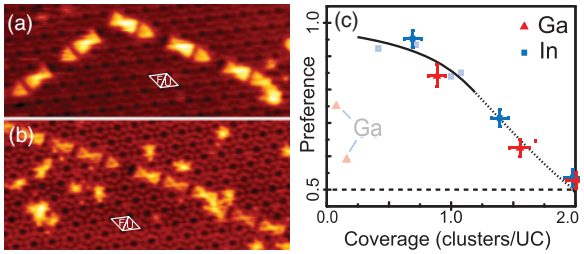

FIG. 5. (Color online) In on B[$\bar{2}$ 2] boundaries at coverage $\phi =$ 1.39 (a), and $\phi = 1.98$ (12×33 nm^2 and 15×33 nm^2). (c) Plot of HUC preference with boundary coverage. Dark points show the preference on B[$\bar{2}$ 2] boundaries. The faint points show the behavior on 7×7, and the trendline is a guide to the eye for In magic clusters on 7×7 adapted from Ref. 18 and references therein.

importantly by the fact that it is a single *unfaulted* half cell.[48] A[0 2] has a higher dangling bond density than B[$\bar{2}$ 2] (0.56 per 1×1 unit cell versus 0.51), but the difference in subsurface stacking sequence is enough to deter cluster formation on this boundary relative to B[$\bar{2}$ 2]. The other boundaries deviate even more strongly from the atomic arrangement required by In and Ga to form stable magic clusters, so their affinity for cluster formation is suppressed even further.

Both In and Ga magic clusters grown on B[$\bar{2}$ 2] maintain their FHUC preference with increasing coverage. Since the B[$\bar{2}$ 2] boundaries collect metal adsorbates from a catchment area defined by the adatom mobility and the proximity of other B[$\bar{2}$ 2] boundaries, the global adsorbate coverage is less important than the local density of domain boundaries. Therefore, as a local measure of coverage we introduce ϕ, the ratio defined by the number of B[$\bar{2}$ 2] clusters divided by the number of available B[$\bar{2}$ 2] UCs: half coverage corresponds to $\phi = 1$, full coverage to $\phi = 2$. Figures 5(a) and 5(b) show B[$\bar{2}$ 2] boundaries with In coverages above half filled. At $\phi = 1.98$ [Fig. 5(b)] essentially all B[$\bar{2}$ 2] HUCS are occupied and the excess In begins to decorate sites within the 5×5 domains. At the boundary, the result is a 1D array of clusters with a lattice defined by the B[$\bar{2}$ 2] periodicity with two oppositely pointing clusters in each unit cell. The center-to-center spacing between two clusters in the same unit cell is the same as that found for fully covered cluster arrays on 7×7 (1.55 nm).[16,17] The spacing of a cluster with its neighbor in the next unit cell is larger (1.77 nm), and the two are separated by the boundary hole which lies between them.

The HUC preference is quantified by $P = f/(f + u)$, where f and u are the fraction of faulted and unfaulted B[$\bar{2}$ 2] HUCs that are occupied by a magic cluster. This definition accounts for the extra or missing HUCs that appear at kinks of the boundary. With equal numbers of F/UHUCs it reduces to the usual definition found in Ref. 18. A plot of preference as a function of coverage [Fig. 5(c)] shows that In and Ga clusters on B[$\bar{2}$ 2] boundaries both maintain a strong preference for FHUC formation and follow the trendline for In clusters on 7×7 proposed in Ref. 18. This enhanced FHUC preference for Ga clusters may be caused by Ge intermixing within the pseudo-7×7 unit cell. This alloying has been previously seen to alter the preferred reconstruction for In overlayers,[51] extend the adsorbate diffusion length,[52] and enhance the stability of Al magic clusters.[53]

We have demonstrated that domain boundaries on Ge/Si(111)-7×7 can be used to template 1D arrays of both In and Ga magic clusters with a lattice constant of 3.33 nm. The strategy we have adopted is to use SPE to grow long straight B[$\bar{2}$ 2] boundaries, that are essentially strips of 7×7 embedded within regions of 5×5. We have taken advantage of the fact that magic clusters do not wet 5×5. Instead, In adatoms move to 7×7 half cells within the B[$\bar{2}$ 2] boundary that are unstable against magic cluster formation.

The templating strategy that we have described above clearly illustrates proof-of-principle for the Ge/Si(111)-7×7 system. However, to take full advantage of the boundaries as templates we clearly need more control of the domain boundary network. As mentioned above, the realization that the regular arrays of steps on vicinal surfaces could be used to template a variety of nanoline structures allowed a large number of 1D systems to be grown. We need an analogous breakthrough for domain boundaries. If the domain boundary networks could be organized into regular arrays, then new surface phases could be fashioned.

Our results, however, clearly demonstrate that there is utility in considering domain boundaries as *features that can be exploited for their unique structural and electronic properties*. This contrasts with the more traditional perspective, that domain boundaries are unwanted structural imperfections.[36,37] We are aware of two other experimental studies that have exploited the properties of domain boundaries, both involving systems that are quite different from Ge/Si(111)-7×7. First, Lahiri *et al.*[54] created extended 1D topological defects, or domain boundaries, in graphene. The boundaries contained octagonal and pentagonal rings and due to doping action, they behaved as 1D metallic wires. Secondly, boundaries between domains of surface adsorbed molecules have been used to confine a second molecular species in a geometry conducive to photoreaction.[55] In this case, the special geometry of the domain boundary makes the regioselective chemistry possible. All three studies mentioned above, exploit the fact that the physical properties of boundary regions are distinct from the properties of the adjacent domains, but to different ends. This suggests that the creation of nanostructured boundary arrays could, in the future, lead to materials with physical properties that could be exploited in devices and sensors.

Financial support was provided by the Natural Sciences and Engineering Research Council of Canada.

*Current address: Max Planck Institute for Intelligent Systems, Heisenbergstrasse 3, Stuttgart 70569, Germany.
†Corresponding author: mclean@physics.queensu.ca; www.physics.queensu.ca/~nanophys

[1] Y. L. Wang and M. Y. Lai, J. Phys.: Condens. Matter **13**, R589 (2001).
[2] J. V. Barth, J. Weckesser, N. Lin, A. Dmitriev, and K. Kern, Appl. Phys. A **76**, 645 (2003).

[3]S. De Feyter and F. C. De Schryver, Chem. Soc. Rev. **32**, 139 (2003).
[4]J. V. Barth, G. Costantini, and K. Kern, Nature (London) **437**, 671 (2005).
[5]J. V. Barth, Annu. Rev. Phys. Chem. **58**, 375 (2007).
[6]C. Becker and K. Wandelt, Top. Curr. Chem. **287**, 45 (2009).
[7]J. A. A. W. Elemans, S. Lei, and S. De Feyter, Angew. Chem. Int. Ed. **48**, 7298 (2009).
[8]A. J. Weymouth, R. H. Miwa, G. J. A. Edge, G. P. Srivastava, and A. B. McLean, Chem Commun. **47**, 8031 (2011).
[9]A. J. Weymouth, G. J. A. Edge, A. B. McLean, R. H. Miwa, and G. P. Srivastava, Phys. Rev. B **84**, 165308 (2011).
[10]J. A. Theobald, N. S. Oxtoby, M. A. Phillips, N. R. Champness, and P. H. Beton, Nature (London) **424**, 1029 (2003).
[11]J. Viernow, J. L. Lin, D. Y. Petrovykh, F. M. Leibsle, F. K. Men, and F. J. Himpsel, Appl. Phys. Lett. **72**, 948 (1998).
[12]J. N. Crain and F. J. Himpsel, Appl. Phys. A **82**, 431 (2005).
[13]P. C. Snijders, Rev. Mod. Phys. **82**, 307 (2010).
[14]P. Gambardella, A. Dallmeyer, K. Maiti, M. C. Malagoli, W. Eberhardt, K. Kern, and C. Carbone, Nature (London) **416**, 301 (2002).
[15]S. C. Erwin and F. J. Himpsel, Nat. Commun. **1**, 1 (2010).
[16]J.-L. Li, J.-F. Jia, X.-J. Liang, X. Liu, J.-Z. Wang, Q.-K. Xue, Z.-Q. Li, J. S. Tse, Z. Zhang, and S. B. Zhang, Phys. Rev. Lett. **88**, 066101 (2002).
[17]J.-F. Jia, X. Liu, J.-Z. Wang, J.-L. Li, X. S. Wang, Q.-K. Xue, Z.-Q. Li, Z. Zhang, and S. B. Zhang, Phys. Rev. B **66**, 165412 (2002).
[18]Y. L. Wang, A. A. Saranin, A. V. Zotov, M. Y. Lai, and H. H. Chang, Int. Rev. Phys. Chem. **27**, 317 (2008).
[19]M. Y. Lai and Y. L. Wang, Phys. Rev. B **64**, 241404 (2001).
[20]H. H. Chang, M. Y. Lai, J. H. Wei, C. M. Wei, and Y. L. Wang, Phys. Rev. Lett. **92**, 066103 (2004).
[21]V. G. Kotlyar, A. V. Zotov, A. A. Saranin, T. V. Kasyanova, M. A. Cherevik, I. V. Pisarenko, and V. G. Lifshits, Phys. Rev. B **66**, 165401 (2002).
[22]J. Jia, J.-Z. Wang, X. Liu, Q.-K. Xue, Z.-Q. Li, Y. Kawazoe, and S. B. Zhang, Appl. Phys. Lett. **80**, 3186 (2002).
[23]S.-C. Li, J.-F. Jia, R.-F. Dou, Q.-K. Xue, I. G. Batyrev, and S. B. Zhang, Phys. Rev. Lett. **93**, 116103 (2004).
[24]J.-Z. Wang, J.-F. Jia, Z.-H. Xiong, and Q.-K. Xue, Phys. Rev. B **78**, 045424 (2008).
[25]A. V. Zotov, D. V. Gruznev, O. A. Utas, V. G. Kotlyar, and A. A. Saranin, Surf. Sci. **602**, 391 (2008).
[26]M. A. K. Zilani, Y. Y. Sun, H. Xu, Y. P. Feng, X.-S. Wang, and A. T. S. Wee, Phys. Rev. B **72**, 193402 (2005).
[27]Z. Zhang and M. Lagally, Science **276**, 377 (1997).
[28]J. Krug, Physica A **313**, 47 (2002).
[29]D. Wang, H. Zhu, L. Wang, and Y. Wu, J. Appl. Phys. **106**, 054315 (2009).
[30]J. M. MacLeod, D. Psiachos, M. J. Stott, and A.B. McLean, Phys. Rev. B **73**, 241306(R) (2006).
[31]D. Psiachos and M. J. Stott, Phys. Status Solidi (b) **245**, 1538 (2008).
[32]N. Kitamura, B.S. Swartzentruber, M.G. Lagally, and M.B. Webb, Phys. Rev. B **48**, 5704 (1993).
[33]W. Xiao, P. Ruffieux, K. Ait-Mansour, O. Groning, K. Palotas, W. A. Hofer, P. Groning, and R. Fasel, J. Phys. Chem. B **110**, 21394 (2006).
[34]J. N. Crain, J. L. McChesney, F. Zheng, M. C. Gallagher, P. C. Snijders, M. Bissen, C. Gundelach, S. C. Erwin, and F. J. Himpsel, Phys. Rev. B **69**, 125401 (2004).
[35]T. Sekiguchi, S. Yoshida, and K. M. Itoh, Phys. Rev. Lett. **95**, 106101 (2005).
[36]T. Berghaus, A. Brodde, H. Neddermeyer, and S. Tosch, Surf. Sci. **193**, 235 (1988).
[37]M. Itoh, H. Tanaka, Y. Watanabe, M. Udagawa, and I. Sumita, Phys. Rev. B **47**, 2216 (1993).
[38]U. Köhler, J. E. Demuth, and R. J. Hamers, J. Vac. Sci. Technol. A **7**, 2860 (1989).
[39]I.-S. Hwang, M.-S. Ho, and T. T. Tsong, Phys. Rev. Lett. **83**, 120 (1999).
[40]N. Sato, T. Nagao, and S. Hasegawa, Phys. Rev. B **60**, 16083 (1999).
[41]R. M. Feenstra, A. J. Slavin, G. A. Held, and M. A. Lutz, Phys. Rev. Lett. **66**, 3257 (1991).
[42]I. Suzumura, M. Okada, A. Muto, Y. Torige, H. Ikeda, A. Sakai, S. Zaima, and Y. Yasuda, Thin Solid Films **369**, 116 (2000).
[43]T. Fukuda, Surf. Sci. **351**, 103 (1996).
[44]F. Rosei, N. Motta, A. Sgarlata, G. Capellini, and F. Boscherini, Thin Solid Films **369**, 29 (2000).
[45]I. Yi, R. Nishi, Y. Sugimoto, M. Abe, Y. Sugawara, and S. Morita, Surf. Sci. **600**, 2766 (2006).
[46]I. Mochizuki, R. Negishi, and Y. Shigeta, J. Appl. Phys. **106**, 013709 (2009).
[47]I. Mochizuki, R. Negishi, and Y. Shigeta, J. Appl. Phys. **107**, 084317 (2010).
[48]A. G. Mark and A. B. McLean, Phys. Status Solidi C **7**, 185 (2010).
[49]P. Y. Huang, C. S. Ruiz-Vargas, A. M. van der Zande, W. S. Whitney, M. P. Levendorf, J. W. Kevek, S. Garg, J. S. Alden, C. J. Hustedt, Y. Zhu *et al.* , Nature (Londoon) **469**, 389 (2011).
[50]J. H. Byun, J. R. Ahn, W. H. Choi, P. G. Kang, and H. W. Yeom, Phys. Rev. B **78**, 205314 (2008).
[51]D. V. Gruznev, D. A. Olyanich, D. N. Chubenko, A. V. Zotov, and A. A. Saranin, Phys. Rev. B **76**, 073307 (2007).
[52]V. Cherepanov and B. Voigtländer, Phys. Rev. B **69**, 125331 (2004).
[53]D. V. Gruznev, D. A. Olyanich, D. N. Chubenko, Y. V. Luniakov, I. A. Kuyanov, A. V. Zotov, and A. A. Saranin, Phys. Rev. B **78**, 165409 (2008).
[54]J. Lahiri, Y. Lin, P. Bozkurt, I. I. Oleynik, and M. Batzill, Nat. Nanotechnol. **5**, 326 (2010).
[55]M. Kim, J. N. Hohman, Y. Cao, K. N. Houk, H. Ma, A. K.-Y. Jen, and P. S. Weiss, Science **331**, 1312 (2011).